LIMNOLOGY and OCEANOGRAPHY

ASLO

Limnol. Oceanogr. 67, 2022, 364–378

doi: 10.1002/lno.11997

Pelagic N_2 fixation dominated by sediment diazotrophic communities in a shallow temperate estuary

Søren Hallstrøm,[1] **Mar Benavides**,[1,2*] **Ellen R. Salamon**,[1] **Clayton W. Evans**,[3] **Lindsey J. Potts**,[4] **Julie Granger**,[4] **Craig R. Tobias**,[4] **Pia H. Moisander**,[3] **Lasse Riemann**[1]

[1]Marine Biology Section, University of Copenhagen, Helsingør, Denmark
[2]Aix Marseille Univ, Université de Toulon, CNRS, IRD, MIO, UM 110, Marseille, France
[3]Department of Biology, University of Massachusetts Dartmouth, North Dartmouth, Massachusetts
[4]Department of Marine Sciences, University of Connecticut Avery Point, Groton, Connecticut

Abstract

Estuaries receive substantial anthropogenic nitrogen loading and are mainly considered net nitrogen sinks. While several studies have identified diverse diazotrophic communities in estuarine sediments, the role of pelagic diazotrophs in these systems is not well understood. We investigated the links between diazotrophic community composition, nitrogenase (*nifH*) gene expression, N_2 fixation, and environmental conditions in Narragansett Bay (USA). Pelagic N_2 fixation rates ranged between 0.02 and 9.41 nmol N L^{-1} d^{-1} and correlated significantly with fluctuations in diazotroph community composition. These fluctuations were also correlated with temperature, salinity, and mean sea level. The dominant sequences in our pelagic samples were related to sequences previously detected in the bay's sediments and were dominated by *nifH* gene Clusters I and III. We interpret this as a coupling between sediment and pelagic diazotroph communities and speculate that resuspension plays an important role for pelagic N_2 fixation in shallow estuarine environments such as Narragansett Bay. For instance, the finding of active sulfate reducers in the oxygenated water illustrates that the sediment-pelagic coupling can impact nutrient cycling in shallow environments. The pelagic N_2 fixation measured during our study period showed only a minor contribution (< 1%) to the total estimated nitrogen load to Narragansett Bay. However, with intensifying nitrogen management in estuaries, the need to constrain the rates of pelagic N_2 fixation in these systems will be essential for estimating nitrogen fluxes within the bay and to the adjacent coastal ecosystems.

The global nitrogen inventory is set by the balance between fixed nitrogen gains in the form of biological dinitrogen (N_2) fixation and losses due to denitrification and annamox, but current measurements of both processes involve large uncertainties (Landolfi et al. 2018). Nitrogen availability fuels the biological carbon pump in otherwise nitrogen-limited systems such as subtropical gyres (Karl et al. 2012), and hence boost the ability of the oceans to cope with excess CO_2 (Hutchins and Fu 2017). Thus, an accurate estimate of N_2 fixation is key to assessing the global ocean's nitrogen inventory and its role in climate regulation.

N_2 fixation represents a central reactive nitrogen supply in warm oligotrophic ocean regions, such as the subtropical gyres (Mahaffey et al. 2005), where dissolved inorganic nitrogen concentrations are typically close to the detection limit and surface temperatures exceed 20°C year round (Luo et al. 2012). Nutrient-rich coastal shelf seas and temperate estuaries were, however, long thought to lack significant diazotrophic activity due to the prevalence of nitrogen-rich inputs from rivers, watershed runoff, and anthropogenic nutrient loading (Howarth et al. 1988; Nixon et al. 1996; Marino et al. 2002). Nevertheless, recent studies have reported high N_2 fixation rates in coastal areas and estuarine environments during periods of low inorganic nitrogen availability. For instance, the shelf waters off the eastern North American coast harbor relatively high N_2 fixation rates and diazotroph communities dominated by unicellular cyanobacteria of group A (UCYN-A), diatom–diazotroph associations, and non-cyanobacterial diazotrophs (Mulholland et al. 2012, 2019; Tang et al. 2019). Moreover, several studies have reported significant N_2 fixation rates and diverse non-cyanobacterial diazotrophic communities in temperate estuaries in Europe, North America, and Australia (Moisander et al. 2007; Bentzon-Tilia et al. 2015*b*; Messer et al. 2021). Still, the potential of coastal and estuarine

*Correspondence: mar.benavides@ird.fr

Additional Supporting Information may be found in the online version of this article.

Søren Hallstrøm and Mar Benavides contributed equally to this study.

environments as a source of bioavailable nitrogen via diazotrophic activity remains unconstrained.

The estuarine Narragansett Bay (USA) covers 370 km^2 and is subject to a semidiurnal tide regime with an average 40-day residence time and seasonally and interannually variable nitrogen-rich freshwater inputs derived via 15 rivers (Nixon et al. 2005). Anthropogenic nitrogen loading has historically driven episodic phytoplankton blooms followed by extensive organic matter deposition to the local seafloor and hypoxic events, particularly in the upper estuary (Bergondo et al. 2005). Organic matter loading induces microbial respiration, which consequently decreases oxygen levels and promotes bacterial denitrification in the sediment. Denitrification converts nitrate to N_2, thereby preventing the delivery of reactive nitrogen to the adjacent coastal ocean (Cornwell et al. 1999). However, the progressive warming observed since the 1970s, and more recently nutrient load management that have reduced effluent inorganic nitrogen inputs by over 50%, have contributed a delay in the winter–spring diatom bloom and a decrease in primary productivity in Narragansett Bay (Nixon et al. 2009; Oviatt et al. 2017). Consequently, the organic matter deposited onto the sediment has progressively decreased in quantity and quality, which has led to a reduction in denitrification rates with reversals to net N_2 fixation activity in the warmest and most nutrient-depleted periods of the year (Fulweiler et al. 2007, 2013). However, a recent study reported N_2 fixation activity related to severe hypoxic events coupled with fresh organic matter inputs in the Bay's sediments (Spinette et al. 2019). The rationale for this process is that hypoxia reduces oxygen availability for nitrification, eventually reducing nitrate concentrations and inhibiting denitrification, providing a niche for diazotrophs to thrive (Spinette et al. 2019). The N_2 fixation activity has been attributed to anaerobic and sulfate-reducing bacteria, which are the dominant diazotrophs in the bay's sediments (Fulweiler et al. 2013; Brown and Jenkins 2014). Similarly, non-cyanobacterial N_2 fixation driven by low oxygen and high organic carbon conditions has been observed in samples collected in a Danish estuary (Severin et al. 2015).

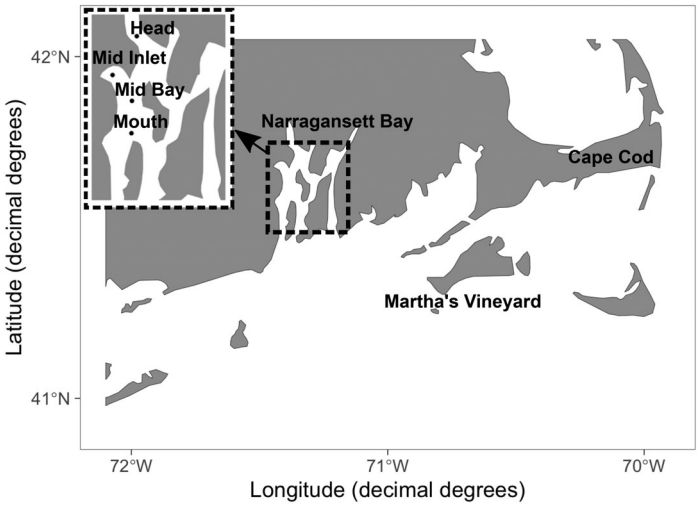

Fig. 1. Sampling area map. The inset indicates the locations of the four sampling stations.

The interplay between N_2 fixing and denitrifying bacterial communities in the sediment impacts nitrogen cycling in estuaries such as Narragansett Bay, influencing the amount of reactive nitrogen that eventually reaches the adjacent coastal ocean. Nevertheless, only few studies have examined microbial nitrogen cycling in the water column of this estuary. Further south, in Chesapeake Bay, diazotrophs include both typical pelagic and benthic taxa suggesting that coastal hydrodynamics, tidal fluxes as well as sediment resuspension affect the composition of planktonic diazotrophs (Short et al. 2004; Moisander et al. 2007). In the present study, we investigated the environmental factors that drive the composition and N_2 fixation activity of the pelagic diazotroph community in Narragansett Bay. To that end, we monitored the diazotroph community composition, nitrogenase (*nifH*) gene expression, and N_2 fixation activity as environmental conditions evolved in late spring through summer, 2017.

Methods

Environmental parameters

Water samples were collected biweekly from 11 May 2017 to 29 August 2017 at four stations along the head to mouth axis of Narragansett Bay (Fig. 1). Samples were collected from the surface ($\sim$ 0.5 m) and just above the seafloor ($\sim$ 4–8 m depending on the station and the tide height; Supporting Information Table S1) using Niskin bottles. Temperature, salinity, dissolved oxygen, and fluorescence (used as a proxy for chlorophyll *a* concentrations) data were obtained by means of a Yellow Springs Inc. probe (YSI, Yellow Springs, OH) casted from the surface to the bottom at each station. Mean sea-level (MSL) data for each date and station were available through the National Oceanic and Atmospheric Administration (https://tidesandcurrents.noaa.gov/; last accessed 10 August 2020).

Samples for nutrient analyses (nitrate, phosphate, and silicate) were collected in 100-mL polyethylene containers and kept on ice until analyses in the lab within the same day. In the lab, samples were filtered through 0.45-μm Nucleopore filters (Millipore, Germany) and analyzed by traditional colorimetric methods on an Astoria SFA nutrient autoanalyzer (Astoria-Pacific, Clackamas, Oregon).

N_2 fixation rates

N_2 fixation rates were measured in triplicate 1.3-L hydrochloric acid-cleaned polycarbonate bottles with water from the surface (clear bottles) and the near bottom (dark bottles), filled to overflow and closed with septum screwcaps. After

transport to the lab (about 3 h, with incubation bottles transported in coolers), each bottle was spiked with 2 mL $^{15}N_2$ gas (98.9 atom %, Cambridge Isotope Laboratories, Tewksbury, Massachusetts), inverted 20–30 times and incubated in temperature- and light-controlled rooms simulating the in situ temperature and diel light cycle. Our choice of the bubble method instead of alternative methods was based on the reasoning that excessive sample agitation or degassing would have affected measurements in the particle-rich waters of the Bay causing larger biases than the potential underestimates associated with the bubble method (White et al. 2020). Previous studies have shown that some $^{15}N_2$ gas batches are contaminated with nitrogen compounds other than N_2, leading to a misinterpretation of nitrate or ammonium uptake as N_2 fixation (Dabundo et al. 2014). While our $^{15}N_2$ gas batch was not specifically tested for contaminations, previous analyses resulted in nearly undetectable levels of contamination and thus do not impact N_2 fixation calculations significantly (Benavides et al. 2015; Moreira-Coello et al. 2019). After 24 h of incubation, 5 mL subsamples of the incubation matrix were transferred into replicate helium-purged Exetainers, which were stored submerged to minimize gas exchange pending analysis of final dissolved $^{15}N_2$ atom % in each incubation (White et al. 2020). The content of the bottles was then filtered onto precombusted (6 h, 450°C) 25-mm Advantec glass fiber filters (nominal pore size 0.3 μm, Cole Parmer, Vernon Hills, Illinois). These filters provide more representative N_2 fixation rates when non-cyanobacterial diazotrophs are dominant (Bombar et al. 2018). The filters were stored at − 20°C until analysis. The concentration of particulate nitrogen (PN) and the isotopic ratio ($^{15}N/^{14}N$) of samples were obtained by means of a Thermo Flash 1112 elemental analyzer interfaced by a Conflo III with a Thermo Delta V Advantage IRMS.

Concentrations of PN ranged between ~ 2 and 17.35 μM, (resulting in ~ 10–100 μg N per filter), within the linearity limit of the IRMS (Supporting Information Table S3). Initial PN samples were filtered upon collection without labeling or incubation to obtain the natural ^{15}N atom % enrichment of PN. Initial PN ^{15}N atom % values were subtracted from those of labeled and incubated samples to calculate N_2 fixation rates. In addition, 20 incubated control samples were also analyzed. These controls were not amended with $^{15}N_2$ but were incubated over the same time period and conditions as labeled samples to account for potential changes of ambient atom % of PN over the incubation period.

The final dissolved $^{15}N_2$ atom % in each incubation was analyzed by Membrane Inlet Mass Spectrometry as detailed in White et al. (2020). These dissolved ^{15}N enrichments ranged between 2.6 and 8.9 atom % (Supporting Information Table S3). The N_2 fixation rates are considered to be conservative given the time-dependence of $^{15}N_2$ dissolution. The range of natural abundance values ($\delta^{15}N$) were 5.59‰ to 11.59‰, while final incubation values were 5.2‰ to 16.5‰. The natural $\delta^{15}N$ variability of control samples (not spiked with $^{15}N_2$ but incubated for 24 h along with labeled samples) represented 1.40% to 10.76% of N_2 fixation rates measured in samples spiked with $^{15}N_2$, meaning that the N_2 fixation rates reported here may be overestimated by up to ~ 11%.

According to the standard propagation of errors via the observed variability between replicate samples (Gradoville et al. 2017), the minimum quantifiable rate ranged between 0.01 and 1.86 nmol N L^{-1} d^{-1} (Supporting Information Table S3).

Nucleic acids sampling, extractions, and *nifH* gene sequencing

Water samples (200–500 mL) for nucleic acids extraction were stored in dark coolers until filtration onto 0.2 μm Supor filters (Pall Gelman, Port Washington, New York), which took place within 2 h of sampling. Filters for DNA extraction were stored in bead beater tubes containing a mixture of 0.1- and 0.5-mm diameter glass beads (BioSpec Products, Bartlesville, Oklahoma). Bead beater tubes containing filters for RNA extraction also contained 350 μL RLT buffer (RNeasy mini kit, Qiagen, Germany) with 1% β-mercaptoethanol. All filters were kept on dry ice during transportation to the lab (within 6 h) and subsequently stored at − 80°C. Samples were then transported to Denmark on dry ice.

DNA was extracted using DNeasy Plant kit (Qiagen) with additional freeze-thaw bead beating and proteinase K steps before purification and elution in 50 μL as previously described (Moisander et al. 2008). RNA was extracted using the RNeasy mini kit with an additional 1 h on-column DNase digestion. Samples were eluted into 50 μL RNase-free water and stored at − 80°C. RNA was reverse transcribed using TaqMan Reverse Transcription reagents (Thermo Fisher Scientific, Waltham, Massachusetts) and reverse primer *nifH*3 (below) with 5 μL of RNA extract. Non reverse transcribed control reactions were run using molecular grade water in place of the reverse transcriptase.

Triplicate, nested polymerase chain reactions (PCRs) were conducted using degenerate *nifH* primers (Zehr and Turner 2001) and the second round primers modified with adapters for Illumina library preparation using a Doppio thermocycler (VWR, Radnor, Pennsylvania). The PCR mix was composed of 5 μL of 5× MyTaq red PCR buffer (Bioline, Meridian Bioscience, UK), 1.25 μL of 25 mM $MgCl_2$, 0.5 μL of 20 μM forward and reverse primers each, 0.25 μL Platinum Taq, and 5 μL of DNA or cDNA extract (1 μL on second round). The reaction volume was adjusted to 25 μL with PCR-grade water. Triplicate PCR products were then pooled and purified using the Geneclean Turbo kit (MP Biomedicals, Germany).

To minimize the risk of amplifying contaminants (Zehr et al. 2003) the PCR preparation station was ultraviolet irradiated for 30 min before and after every usage. Negative

controls (autoclaved and ultraviolet-irradiated water) were run with every PCR experiment and despite no visible PCR products were detected, these were treated as the samples, and included in the sequencing. No sequences were obtained.

The purified products were indexed using custom designed Illumina indexes (Swedish National Genome Institute [NGI], Sweden) that were attached to the specific *nifH* PCR products by an 8-cycle PCR using similar PCR conditions as above and 5 μL of the purified product obtained from the nested PCR reactions as template. Indexed products were purified (AMPure XP beads, Agencourt, Beckman Coulter, Brea, California), quantified (PicoGreen, Thermo Fisher Scientific), adjusted to equimolar concentrations, and pooled for multiplex sequencing on Illumina MiSeq 2×300 bp paired-end sequencing platform (NGI, Stockholm facility, Sweden). Sequences have been deposited in the Sequence Read Archive under accession number PRJNA656687.

Sequence and phylogenetic analyses

Raw demultiplexed paired-end sequences were processed into amplicon sequence variants (ASVs) using DADA2 (Callahan et al. 2016) implemented in R-4.0.3. The parameters for DADA2 "filterandTrim" were: truncLen = c(220,180), maxN = 0, maxEE = c(2,5), truncQ = 2, m.phix = TRUE, trimLeft = 17. Primer sequences were removed by trimLeft, that is, first 17 bps of the forward and reverse reads. Denoised reads were merged and chimeric sequence mergers removed using the functions "mergePairs" and "removeBimeraDenovo." Only sequences with a length of 325–330 bp were kept. Samples with less than 1000 reads were removed. The generated ASVs were translated to amino acid sequences using FrameBot (Wang et al. 2013) and filtered for homologous genes using the NifMAP pipeline (Angel et al. 2018). No homologous genes were observed. Taxonomic ranks were assigned with DIAMOND blastp (Buchfink et al. 2014) using a FrameBot translated *nifH* database (Moynihan 2020) based on the ARB database from the Zehr Lab (version June 2017; https://www.jzehrlab.com/nifh). Relationship to the canonical *nifH* clusters (Zehr et al. 2003) were assigned according to Frank et al. (2016). Nucleotide sequences of the top 50 most abundant ASVs were queried against the NCBI non-redundant database using BLAST and information regarding the environment of isolation for the nearest relative was extracted (Supporting Information Table S2). Amino acid sequences of the top 50 ASVs were aligned with the nearest cultivated relatives determined by FrameBot, nearest relatives in GenBank, and selected translated sequences of expressed *nifH* obtained from Narragansett Bay sediments (Fulweiler et al. 2013) using MAFFT (Katoh et al. 2018). A maximum likelihood phylogenetic tree was constructed using RAxML (Kozlov et al. 2019) and visualized with iTOL (Letunic and Bork 2019). For sequences annotated as UCYN-A, sublineages were assigned by determining the phylogenetic relationship to UCYN-A reference sequences (Farnelid et al. 2016; Turk-Kubo et al. 2017).

Quantitative PCR of UCYN-A2

UCYN-A2, the most abundant cyanobacterium among the *nifH* amplicons, was quantified using TaqMan quantitative PCR (qPCR) assay (Thompson et al. 2014). The qPCR was run in 12.5 μL reactions that consisted of 6.25 μL TaqMan PCR Master Mix (Applied Biosystems, Invitrogen), 0.25 μL of the forward and reverse primers (10 μM, TAG Copenhagen, Denmark), 0.125 μL probe (10 μM, TAG), 4 μL PCR-grade water, 0.63 μL bovine serum albumin (10.08 $\mu g\,\mu L^{-1}$), and 1 μL standard or sample (samples were prediluted to 5 ng μL^{-1} to add 5 ng DNA to all qPCRs). The qPCRs (2 min at 50°C, 10 min at 95°C, then 45 cycles of 15 s at 95°C and 1 min at 64°C) were run on a Stratagene Mx3005P thermal cycler (Applied Biosystems). Standard dilutions (10^1–10^8 gene copies) were run in duplicate, and samples and no-template controls in triplicate. The no-template controls did not show any amplification. The efficiency was 103% to 113%. Inhibition tests were carried out on all samples by adding the 10^4 standard to each sample. The inhibition was between 0.04% and 6.16% (average 3.2%). The limit of detection (LOD) and detected but not quantifiable (DNQ) limits used were one and eight gene copies per reaction. DNQ matches the lowest standard and corresponds to 1421 copies L^{-1} seawater.

Data analysis

Statistical analyses were performed using the software PRIMER-6 with permutational analysis of variance (PERMANOVA) add-on (Clarke et al. 2014) or in R-4.0.3. Sequence abundance tables for both DNA and RNA were square root transformed prior to building Bray–Curtis dissimilarity matrices unless otherwise mentioned. Environmental parameter values were normalized to zero median and unit variance (*z*-scores) prior to all analyses following a "nearest-neighbor" imputation of missing values using the function "knnImputation" of the package "DMwR2" (v. 0.0.2; Torgo 2016). Overall environmental differences were calculated as standardized Euclidean distances between samples considering all measured variables. For correlation analysis of the 50 most abundant ASVs, N_2 fixation rates, and MSL, a centered log-ratio transformation was applied on the ASV count table. All Spearman correlation analyses were done using the function "corr.test" from the package "psych" (v. 2.1.3; Revelle 2021). Differences in microbial community composition were illustrated by nonmetric multidimensional scaling (NMDS) using the package "phyloseq" (v. 1.32.0; McMurdie and Holmes 2013) and environmental vectors were calculated by "envfit" of "vegan" (v. 2.5.6; Oksanen et al. 2019). All plots were generated using "ggplot2" (v. 3.3.3; Wickham 2016). Statistical analyses were performed with compositional data based on the "total sum" relative read abundances, except for the correlation analysis of UCYN-A2 gene counts with

environmental variables. Map of Narragansett Bay with sampling stations was produced with the R package "ggOceanMaps" (v. 1.1; Vihtakari 2020).

Results

Spatiotemporal distribution of environmental parameters

A pronounced salinity gradient was observed with surface values close to 20 at the Head station under the influence of the Providence River, increasing toward the Mouth where salinity reached 31.2 (Supporting Information Fig. S1). Water temperatures ranged from 12°C to 24°C during our sampling period, specifically between 12°C and 14°C in May, and between 14°C and 17.5°C in early June. For the rest of the sampling period, the water column showed temperatures above 20°C, being lowest at the Head station and increasing toward the Mouth station (Supporting Information Fig. S2). The vertical water temperature and salinity profiles, and resulting water density profiles (Supporting Information Fig. S3), suggested that the water column was well mixed, except at station "Head" in May and June, where freshwater inflow generated density gradients resulting in a stratification of the water column. The degree of water column mixing at the Head station increased from May to late August, as revealed by increasingly uniform salinity and density profiles (Supporting Information Figs. S1, S3). Spatiotemporal differences in inorganic nutrient concentrations were observed in surface waters across the study period (summarized in Supporting Information Table S1). Highest nitrate concentrations were measured on 11 May with the highest overall value of 20.32 μM at the "Head" station, which decreased to 1.57 μM on 9 June. In the same period, the nitrate concentration at the "Mid Bay" station increased from 9.08 to 18.76 μM before decreasing to 4.63 on 28 June. The nitrate concentrations at the "Mid Inlet" and "Mouth stations" were always much lower and often below limit of detection. The measured phosphate concentrations displayed a strikingly similar pattern. For both nitrate and phosphate, a general decreasing trend was seen along the study period from spring to late summer.

Concentrations of dissolved oxygen ranged between 4 and 11 mg L^{-1} (Supporting Information Fig. S4). Taking salinity and temperature differences into account this corresponds to 45% and 100% air saturation, respectively. The greatest differences between the surface and the bottom were at the Mid Inlet station, while the rest of stations showed more uniform values with depth. Dissolved oxygen concentrations were lowest at the Head, especially in July where concentrations reached ~ 5 mg L^{-1} throughout the water column (Supporting Information Fig. S4D,E). However, it should be noted that dissolved oxygen concentration is subject to diurnal changes (Guasch et al. 1998), and the observed differences may thus be influenced by changes in sampling time (Supporting Information Table S1).

Chlorophyll concentrations, estimated by fluorescence measurements, showed great variability during the sampling period, ranging between 0.4 and ~ 28 μg L^{-1}. Typically, Chlorophyll concentrations were higher at the Head station and decreased toward the Mouth, decreasing from surface to bottom (Supporting Information Fig. S5).

N_2 fixation activity

N_2 fixation rates were significantly higher in surface samples compared to deep samples (t test, $p = 0.01$), ranging between 0.08 ± 0.09 and 9.41 ± 4.61 nmol N L^{-1} d^{-1}, and between 0.02 ± 0.002 and 5.29 ± 1.60 nmol N L^{-1} d^{-1} in surface and deep samples, respectively. N_2 fixation rates were generally highest at the surface samples at the head (Fig. 2). N_2 fixation rates differed significantly between stations (one-way ANOVA, $p < 0.05$), but not between sampling dates or depths. Spearman rank correlations revealed a significant positive correlation between N_2 fixation rate and chlorophyll ($r_s = 0.50$, $p < 0.001$), but N_2 fixation rate was not significantly correlated to any other environmental variables.

Diazotroph community composition and responses to environmental variability

Amplicon sequencing of nitrogenase genes (*nifH*) was employed to gain insight into the diazotroph community composition of present (DNA) and active (mRNA) diazotrophs. A total of 10,968,183 reads were obtained from the 54 DNA and 28 RNA samples, yielding $\sim$ 2000–333,000 reads per sample (average $\sim$ 84,000). A total of 28,097 ASVs were generated. The *nifH* sequence libraries were dominated by sequences classified as *nifH* Cluster I (54% DNA; 63% RNA) and Cluster III (45% DNA; 36% RNA). The diazotroph community was dominated by non-cyanobacterial diazotrophs across all samples (Fig. 3). Sequences annotated as Deltaproteobacteria accounted for the majority of reads, with 69% of all DNA and 56% of mRNA reads. Overall, cyanobacterial sequences only comprised a minor part of the *nifH* sequence data. In total, 234 ASVs (0.8%) were classified as cyanobacteria, accounting for a total of 1.2% of DNA sequences and 2.9% of mRNA sequences. The diazotroph community composition displayed fluctuations along the study period (Fig. 3A). Interestingly, the expression profiles of the community appeared more stable (Fig. 3B). Indeed, the variation in the composition of diazotrophs (DNA) was higher than the variation in expressed *nifH* genes (RNA; PERMANOVA, $p < 0.001$; Supporting Information Fig. S6).

The composition of diazotrophs differed between both sampling months and stations (PERMANOVA, $p < 0.0001$), and, to a lesser degree, sampling depth (PERMANOVA, $p < 0.05$). Using distance-based linear modeling (DistLM), we found that the differences in diazotroph community composition correlated significantly with several environmental parameters (Fig. 4A), namely temperature ($p < 0.01$), salinity ($p < 0.05$), dissolved oxygen ($p < 0.01$), chlorophyll ($p < 0.01$),

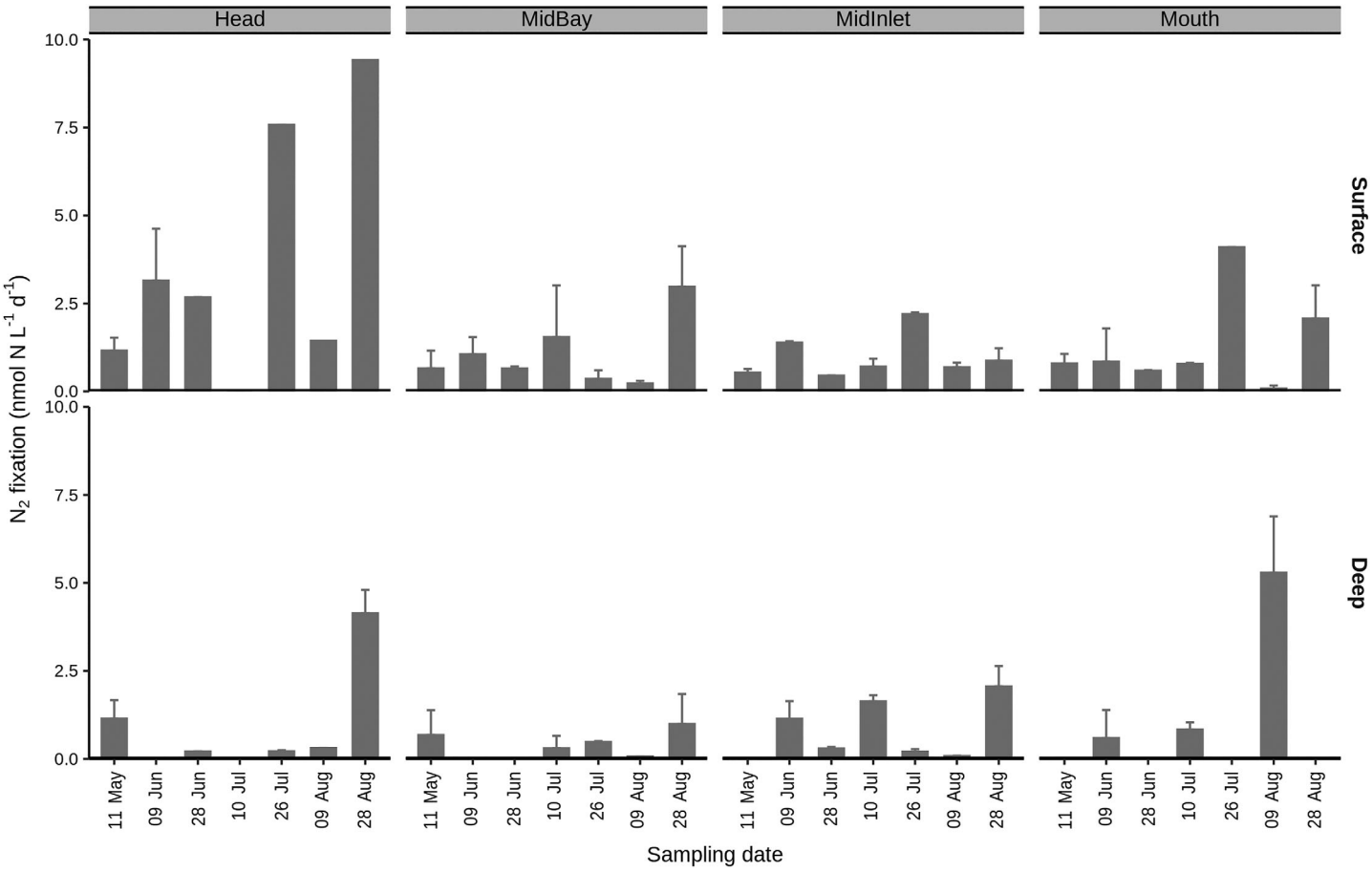

Fig. 2. N_2 fixation rates measured from 11 May 2017 to 29 August 2017. The rates shown are from surface (~ 0.5 m) and deep-water samples (4 - 8 m, depth varies depending on tide height, see Supporting Information Table S1). Error bars represent the standard deviation of the mean from three experimental replicates.

and MSL ($p < 0.01$), as well as N_2 fixation rate ($p < 0.01$). We recovered sequence data for *nifH* gene expression from late May to early June. The pattern of *nifH* expression differed significantly between the sampling depths (PERMANOVA, $p < 0.05$). Interestingly, *nifH* expression in both surface and deep waters was not influenced by sampling location but rather by sampling month (PERMANOVA, $p < 0.05$) and correlated significantly with temperature ($p < 0.01$). The pattern of *nifH* expression did not correlate with any of the other environmental parameters measured (Fig. 4B).

Detailed analysis of the most abundant ASVs and predominant groups

Further phylogenetic and environmental characterization was performed for the 50 most abundant ASVs across all samples, representing 38% and 39% of all reads obtained from DNA and RNA samples, respectively. A correlation analysis of centered log-ratio normalized relative abundances and normalized N_2 fixation rates and MSL did not reveal any significant patterns between the most abundant ASVs and these variables (data not shown). Next, a phylogenetic tree was constructed with the 50 most abundant ASVs, nearest relatives obtained from GenBank, FrameBot targets, and additional reference sequences (Supporting Information Fig. S7). Notably, the majority of the most abundant ASVs that were obtained from the water column clustered closely with expressed *nifH* sequences obtained previously from the sediments of Narragansett Bay (designated NB in Fig. S7; Fulweiler et al. 2013) and shared a high sequence similarity at the amino acid level (> 98% overall similarity; alistat v. 1.3; Jayaswal et al. 2014).

Twenty of the 50 most abundant ASVs were classified as *nifH* Subcluster 1A and in the complete sequence data set Subcluster 1A comprised 37% and 33% DNA and mRNA reads, respectively. This subcluster included ASV1, which showed the highest relative abundance across all samples. The FrameBot targets in this subcluster were strictly anaerobic bacteria including the Deltaproteobacteria *Pelobacter carbinolicus* and *Desulforomonas acetoxidans*. Cluster III sequences related to facultative or obligate anaerobe Deltaproteobacteria, including *Desulfovibrio*, *Pseudodesulfovibrio*, and *Desulfobacter*, were

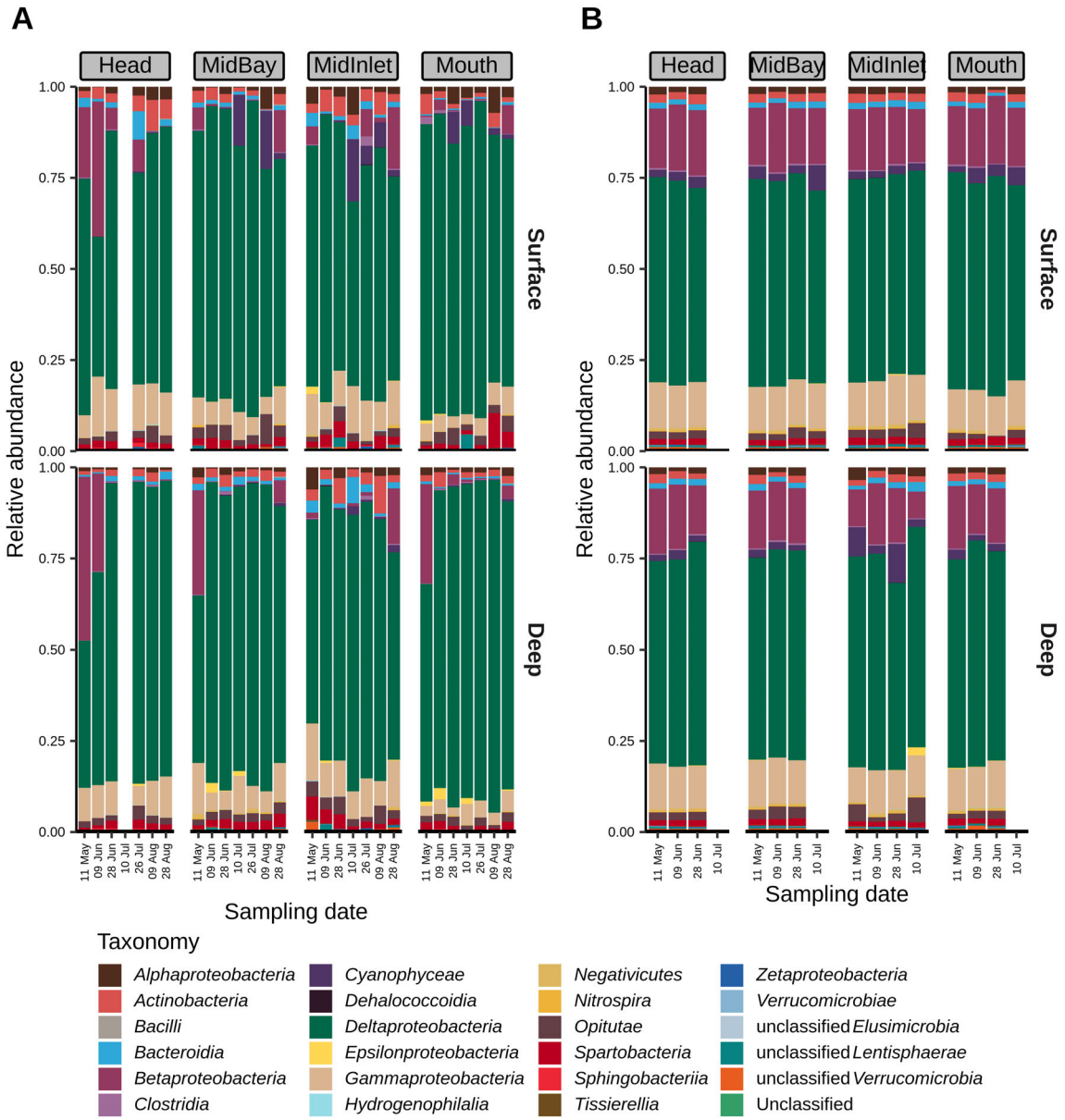

Fig. 3. Relative abundance at a class level of *nifH* DNA (**A**) and mRNA (**B**) observed in samples obtained from surface (~ 0.5 m) and deep (4 - 8 m, depth varies depending on tide height, see Supporting Information Table S1) at four stations in Narragansett Bay during spring and summer 2017.

also prominent among the top 50 ASVs. These observations led us to investigate the environmental origin of the nearest relatives in GenBank for the 50 most abundant ASVs (Fig. 5). In total, 34 of the 50 nearest relatives were highly similar to sequences of uncultivated diazotrophs recovered from sediments of Narragansett Bay (87–100% similarity, average 97.8%), and to the sediments of other temperate marine environments such as the Bohai Sea, South China Sea, and North Sea (Supporting Information Table S2). The majority of these sediment-related sequences were classified as Deltaproteobacteria (29 in total [85%]; Supporting Information Fig. S8). Overall, the sediment-related sequences dominated both the diazotroph community (Fig. 5A) and expression profiles (Fig. 5B) of the 50 most abundant ASVs. Taken together, the majority of the dominant *nifH* sequences obtained from the water column of Narragansett Bay were closely related to sediment derived diazotrophs and highly similar or even identical to active diazotrophs previously reported from the local sediments (Fulweiler et al. 2013). A noteworthy exception was ASV50, found in Subcluster 1G on the *Pseudomonas*/*Vibrio* branch, where the nearest relatives originate from coastal waters. Subcluster 1G is generally dominated by pelagic Gammaproteobacterial sequences and comprised a total of 6% and 7% of DNA and mRNA reads, respectively.

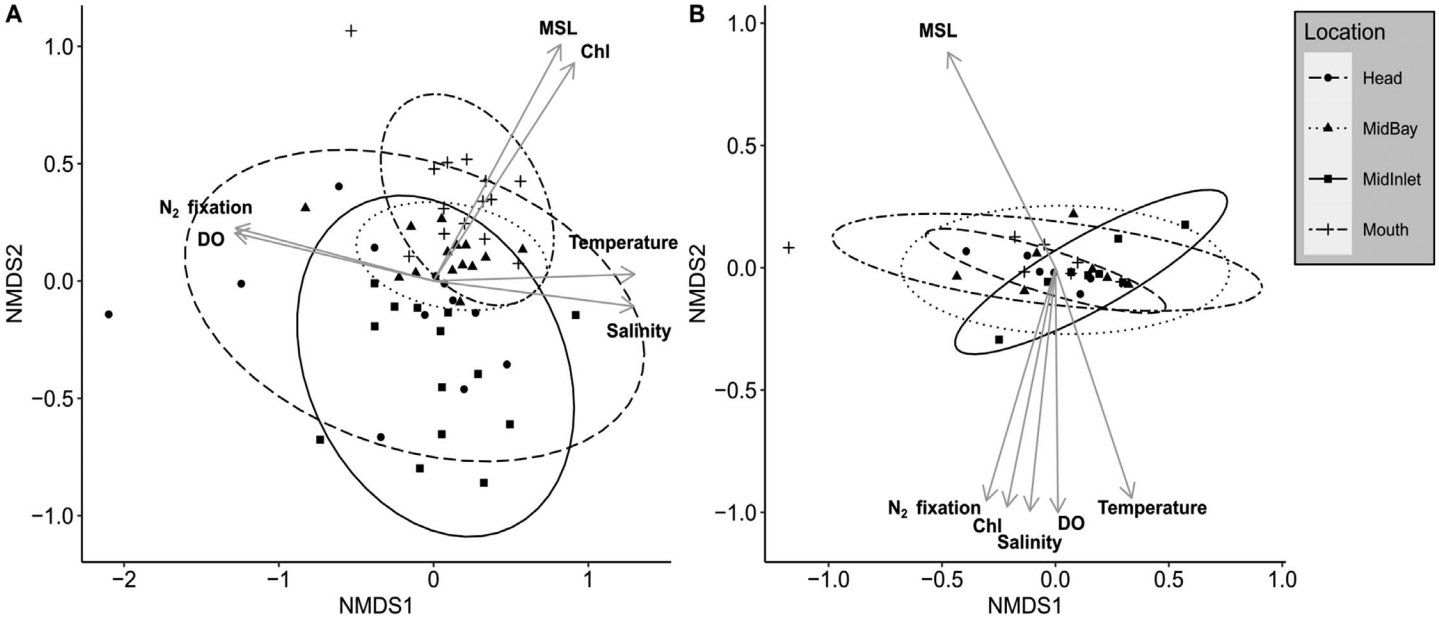

Fig. 4. Relationship between environmental parameters and diazotroph community composition or *nifH* expression profiles. Non-metric multidimensional scaling of the Bray Curtis dissimilarity of (**A**) community composition (DNA, stress 0.152), and (**B**) expression profiles (mRNA, stress 0.074) of the diazotroph community of Narragansett Bay. Correlation vectors show N_2 fixation rates and environmental variables (chlorophyll [Chl; estimated by fluorescence], temperature, salinity, dissolved oxygen [DO], and mean sea level [MSL]).

Four of the 50 ASVs were classified as *nifH* Subcluster 1P and were distantly related (< 95% similarity) to sequences of uncultivated diazotrophs obtained from soil and accounted for 7% of all DNA reads. Especially at the "Head" station they constituted a considerable fraction of the diazotroph community and their occurrence appeared to be associated with the observation of density gradients at the "Head" station (Supporting Information Fig. S3). On 9th June, Subcluster 1P sequences accounted for up to 75% of recovered sequences for the 50 most abundant ASVs (Fig. 5A). In contrast, they were virtually undetected in samples obtained at the MidBay and MidInlet stations between 9th June and 9th August. Interestingly, however, these soil-associated phylotypes constituted a persistent portion of the expression profiles, averaging ~ 20% across all mRNA samples for the 50 most abundant ASVs (Fig. 5B) and overall Subcluster 1P comprised 17% of all mRNA reads.

ASV7, annotated as *Candidatus* Atelocyanobacterium thalassa (UCYN-A), was the only ASV annotated as Cyanobacteria among the top 50 ASVs. Analysis of the phylogenetic relationship to reference UCYN-A sequences (Farnelid et al. 2016) revealed that ASV7 belonged to the sublineage UCYN-A2 (100% identical to UCYN-A2 at the nucleotide level, 95% identical to both UCYN-A1 and UCYN-A3 reference sequences). ASV7 was identical at the amino acid level to the phylotypes NB_50 and NB_51, earlier found as transcripts in Narragansett Bay sediments (Fulweiler et al. 2013).

Abundance and distribution of ASV7 (UCYN-A2)

Given that ASV7 (UCYN-A2) was among the dominant ASVs in DNA (1.0% of reads) and RNA (1.7% of reads), and was the only prevalent diazotrophic cyanobacterium, we performed a detailed analysis to investigate its distribution, dispersal and potential role in N_2 fixation activity. ASV7 was present in DNA samples throughout the sampling period, and in all mRNA samples from which sequences were recovered (from 11th May to 28th June). In surface waters, the relative abundance at the DNA level was influenced by the time of sampling (PERMANOVA, $p < 0.05$) and correlated with temperature and salinity (DistLM, $p < 0.05$). In deep samples, there was a correlation with temperature ($p < 0.05$), but there was neither effect of sampling month nor location. A similar pattern was found for the relative abundance of ASV7 in mRNA, with highest relative abundances at the Mid Inlet and Mid Bay stations. In surface waters, the mRNA abundance was influenced by sampling time and location (PERMANOVA, $p < 0.05$) and was positively correlated to changes in MSL and dissolved oxygen ($p < 0.01$), but not to any of the other environmental parameters. Neither effects of sampling time or location, nor correlation to environmental parameters was observed in the deep samples. Surprisingly, for both DNA and mRNA, no difference was found in relative abundance between surface and deep samples. Interestingly, N_2 fixation rates did not correlate with the relative abundance of ASV7 in either DNA or mRNA.

To assess the distribution of UCYN-A2 and further examine its role in the local N_2 fixation its abundance was estimated by qPCR. The copy numbers exceeded the limit of quantification (8 *nifH* copies per reaction) in 23 out of 54 samples. The abundance of UCYN-A2 *nifH* gene copies ranged from

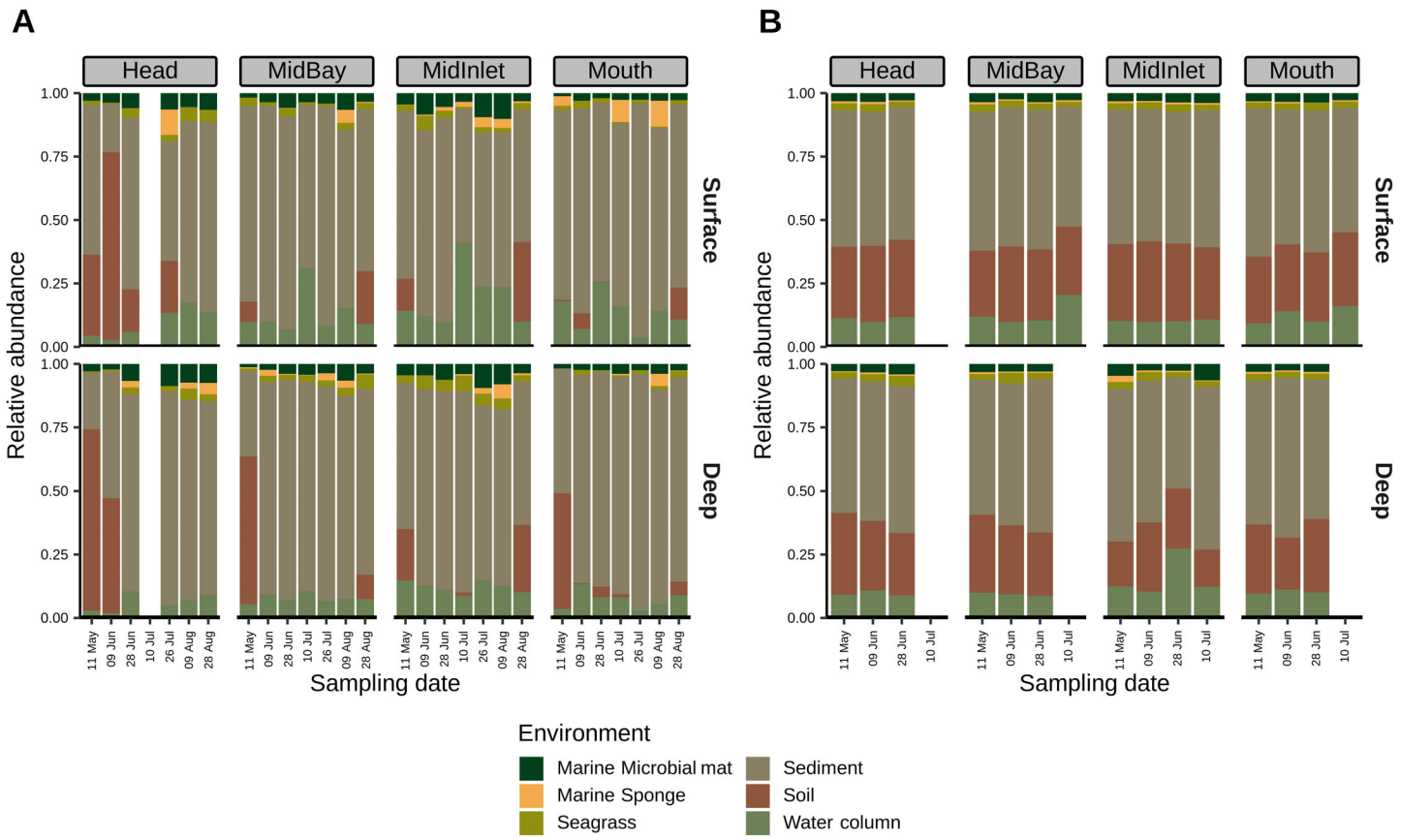

Fig. 5. The environmental origin of the nearest relatives in GenBank for the 50 most abundant ASVs, in either the diazotroph community (**A**) or expression profiles (**B**), observed in samples obtained from surface (~ 0.5 m) and deep (4 - 8 m, depth varies depending on tide height, see Supporting Information Table S1). Accession numbers for the nearest relatives are listed in Supporting Information Table S2.

1 (conservative estimate for detected but not quantifiable) to 9.3×10^6 *nifH* gene copies L^{-1}, and was positively correlated to the relative abundance of ASV7 in the *nifH* amplicons (Spearman rank correlation, $p < 0.0001$). More samples were quantifiable in surface (19) than in deep waters (14), with total absence in deep waters in May (Supporting Information Fig. S9A) and maximum abundance in late June and early July (Supporting Information Fig. S9C,D). However, across all samples there was a positive correlation between *nifH* gene copies of UCYN-A2 in surface and deep samples ($p < 0.001$). The UCYN-A2 copy abundance L^{-1} was correlated with MSL in both surface ($p < 0.05$) and deep ($p < 0.01$) waters. However, no correlation was found to N_2 fixation activity or chlorophyll ($p = 0.14$ and $p = 0.77$).

Discussion

Pelagic N_2 fixation is dominated by non-cyanobacterial diazotrophs of benthic origin

Here, we show that N_2 fixation takes place in the water column of the eutrophic and estuarine Narragansett Bay, at rates comparable to previous open ocean measurements in the North Atlantic (Luo et al. 2012) as well as to rates obtained from similar eutrophic temperate environments such as the Dutch coast line (Fan et al. 2015) and Danish fjords (Bentzon-Tilia et al. 2015*a*; Pedersen et al. 2018), and subtropical and tropical environments such as the Amazon River plume (Subramaniam et al. 2008), the Eastern Arabian Sea (Ahmed et al. 2017; 2019), and the Qishon River (Geisler et al. 2020). In line with results of several of these studies, our data indicate that non-cyanobacteria are responsible for the N_2 fixation, but strikingly, our analysis revealed that these dominant and active diazotrophs were similar or even identical to phylotypes found earlier in local sediments. These findings points to an important benthic-pelagic coupling of diazotrophic communities in Narragansett Bay. The extent to which this is a general phenomenon in shallow estuaries remains to be explored.

The extensive environmental dynamics of temperate estuaries are thought to affect the composition of local diazotroph communities (Fan et al. 2015; Bentzon-Tilia et al. 2015*b*) and the observed variability of the pelagic diazotroph community composition suggested marked responses to the environmental fluctuations in Narragansett Bay. Nevertheless, the

composition of active diazotrophs (expressing *nifH*) remained surprisingly stable over our sampling period, especially in surface waters. An example of this is the occurrence of soil-derived diazotrophs, that at the "Head" station comprised a substantial part of the community in May and June, coinciding with water column density gradients suggesting these might be introduced to the bay via riverine outflow of freshwater, but comprised a stable part of the transcription profiles at all stations. These puzzling and seemingly contrasting observations may be reconciled in a scenario where different environmental factors control expression rather than distribution of *nifH* phylotypes, as earlier suggested for Chesapeake Bay (Short and Zehr 2007). It may then be speculated that for some *nifH* phylotypes the ability to fix N_2 does not represent a strong selective driver.

Many of the dominant diazotrophs observed in the water column during our sampling were affiliated with *nifH* Subcluster 1A and Cluster III. These sequence clusters contain putative anaerobic diazotrophs previously observed in the Bay's sediments (Fulweiler et al. 2013; Brown and Jenkins 2014; Spinette et al. 2019) as well as in other temperate and subtropical estuarine systems (Moisander et al. 2007; Bentzon-Tilia et al. 2015*b*). The reports of active non-cyanobacterial diazotrophs in eutrophic coastal and estuarine environments, coupled with molecular evidence of the genetic basis for how heterotrophic bacterial diazotrophs can maintain N_2 fixation under high nitrogen conditions (reviewed in Bombar et al. 2016), suggests that eutrophic environments may be a niche for non-cyanobacterial diazotrophs. Furthermore, the reduced light availability in turbid estuaries influenced by sediment resuspension might favor non-cyanobacterial diazotrophs over diazotrophic cyanobacteria. The expression of *nifH* mRNA originating from putative anaerobic bacteria in the Narragansett Bay water column suggests co-occurring low oxygen conditions. However, since the water column was always oxic during the sampling period (Supporting Information Fig. S3), we speculate that the putative anaerobic diazotrophs detected benefitted from oxygen-depleted and organic matter-rich conditions found in pelagic particles (Riemann et al. 2010; Pedersen et al. 2018; Chakraborty et al. 2021). Such particles may be formed by aggregation of phytoplankton biomass and/or resuspended from the sediment. The high degree of water column mixing observed during our study (Supporting Information Fig. S3) does not allow discerning between these two options. However, since N_2 fixation activity was positively correlated with fluorescence in the deep samples, and sediment derived diazotrophs were widespread in these samples, we speculate that resuspension of phytoplankton biomass deposited on the sediments could have contributed to the diazotroph activity in the deep waters.

We consider that the active pelagic diazotrophs were predominantly of sediment origin since the dominant non-cyanobacterial diazotrophs among the top 50 ASVs were closely related to sediment bacteria (Fig. 5). The obtained density profiles show that the water column was well mixed at the majority of sampling points and supports that sediment resuspension was physically possible. Furthermore, a majority of the 50 most abundant ASVs exhibited high sequence similarity (> 98%) with expressed *nifH* sequences from sediment samples previously reported in samples near the Mid Bay station of Narragansett Bay (Fulweiler et al. 2013). Similarly, other studies have reported the presence of typical sediment diazotrophs in shallow coastal waters of the North Sea (Fan et al. 2015), Baltic Sea region (Bertics et al. 2013; Bentzon-Tilia et al. 2015*b*), and the Great Barrier Reef (Hewson et al. 2007). Indeed, it has been suggested that sediment resuspension can influence the composition of pelagic diazotrophic communities in shallow waters (Moisander et al. 2007; Pedersen et al. 2018; Zilius et al. 2020), and may even stimulate N_2 fixation (Pedersen et al. 2018). Sediment resuspension due to tidal currents and winds is well known to affect the activity and composition of pelagic microbial communities in shallow coastal ecosystems (Porter et al. 2010; Guizien et al. 2014). However, our finding of prevalent and active sediment derived diazotrophs in the water column presents a new perspective by suggesting that physical forcing upon sediments affects pelagic diazotroph communities and possibly N_2 fixation. Supporting this idea, the MSL, which we use as a proxy for tidal dynamics, exerted a significant effect on the variability of diazotroph community composition (Fig. 4).

Phytoplankton biomass in or on the sediment likely provided the organic matter needed by the heterotrophic diazotrophs, including anaerobic sulfate reducing Deltaproteobacteria (Fig. 3; Supporting Information Fig. S7). Indeed, we found a positive correlation between chlorophyll and N_2 fixation rates, and a significant effect of chlorophyll levels on the diazotroph community composition. This may suggest that diazotrophs were associated with chlorophyll-rich particles that at least partially derive from phytoplankton biomass previously deposited onto the sediments. This is consistent with a previous study in Narragansett Bay sediments showing N_2 fixation stimulated by organic matter inputs (Spinette et al. 2019) and the sampling period of the present study coincided with the highest chlorophyll concentrations observed along the year in Narragansett Bay (Oviatt et al. 2002). Similar results have been obtained from pelagic tropical and temperate coastal ecosystems, as well as in deep aphotic waters (Moisander et al. 2014; Benavides et al. 2015; Severin et al. 2015). The reduction in anthropogenic nutrient loading and long-term increases in temperature have caused a decline of phytoplankton blooms and a decrease in the quality of the organic matter deposited in Narragansett Bay (Codiga et al. 2009; Oviatt et al. 2017), leading to a reduction in denitrification and an expansion of the niche for diazotrophic activity (Fulweiler et al. 2007, 2013). The balance between organic matter loading, oxygen consumption, and denitrification/N_2 fixation in this system is complex and varies with season, but could explain the ubiquity of bacteria with a dual

denitrification and N_2 fixation ability such as *Pseudomonas stutzeri* in the bay's sediments (Fulweiler et al. 2013; Brown and Jenkins 2014) and in other estuarine environments (Bentzon-Tilia et al. 2014, 2015*a*). Indeed, we detected *nifH* genes and transcripts of a phylotype closely related to *P. stutzeri* in our water column samples (Supporting Information Fig. S7). Moreover, the finding of active sulfate reducers in the oxygenated water further shows that the sediment-pelagic coupling may affect nutrient cycling in shallow environments.

While our samples were dominated by non-cyanobacterial diazotrophs, we recovered an ASV which was identical at the nucleotide level to the unicellular cyanobacterium UCYN-A2 (ASV7). This sublineage of UCYN-A is abundant in the eastern North American coastal shelf waters (Mulholland et al. 2012, 2019), which may suggest it is advected from the adjacent coastal waters into the bay. However, the UCYN-A2 sequence was identical at the amino acid level with expressed *nifH* genes obtained from sediments of Narragansett Bay (Fulweiler et al. 2013), even at locations distant from the estuary's mouth (Brown and Jenkins 2014). Similarly, UCYN-A2 sequences have been detected at intermediate distances from the adjacent coastal ocean in an inverse estuary in Southern Australia (Messer et al. 2021). In our study, most of the UCYN-A2-related sequences were recovered from the Mid Inlet and Mid Bay stations, and UCYN-A2 could occasionally be quantified at all stations in summer (Supporting Information Fig. S9). According to the circulation patterns of the bay, coastal waters enter through the east passage (east of the islands, Fig. 1), turning to the west and flowing south along the west passage (Rogers 2008). This pattern could explain the presence of coastal UCYN-A2 at stations even distant from the mouth of the estuary. We found that the MSL was positively correlated with the *nifH* mRNA levels of ASV7, suggesting that the activity of ASV7 in the bay is affected by tidal dynamics. Interestingly, the eukaryotic host of UCYN-A2, *Braarudosphaera bigelowii*, shifts between a calcified non-flagellar form in the sediment and an uncalcified flagellated pelagic form when favorable environmental conditions are sensed (Hagino et al. 2016). We speculate that the symbiosis could be a permanent resident of the bay and is seeded from the sediment into the water column. Indeed, a recent study suggested this mechanism to explain the presence of UCYN-A2 in the water column of Monterey Bay (California) over the summer months, and its absence during winter months (Cabello et al. 2020). Further studies of the calcification dynamics of the host and its presence in coastal sediments are needed to confirm this hypothesis. In any case, despite that UCYN-A2 *nifH* mRNA was detected over an extended part of our sampling period, the *nifH* copy numbers did not correlate with N_2 fixation rates, suggesting a minor contribution to the measured rates.

In conclusion, we mainly attribute the N_2 fixation activity in the waters of Narragansett Bay to heterotrophic diazotrophs. Our data suggest a tight sediment-pelagic coupling and we speculate that resuspension events play an important role for pelagic N_2 fixation. However, disentangling the patterns of these abrupt and ephemeral events requires dedicated turbidity, current and wind dynamics analysis in future studies.

Pelagic N_2 fixation contributes minimally to nitrogen loading in Narragansett Bay

Narragansett Bay is a highly dynamic environment, influenced by multiple environmental factors such as runoff, anthropogenic nitrogen loading, and freshwater input from rivers and salt water inputs that invade the bay through a semidiurnal tide regime (Li and Smayda 1998). Nitrogen loading has decreased notably over the past decades (Oczkowski 2018), which may provide a spatiotemporally variable niche for diazotrophs in Narragansett Bay as well as in other nitrogen loading managed estuaries (Fulweiler et al. 2007; Messer et al. 2021). Indeed, we found measurable N_2 fixation rates in the bay (0.02–9.41 nmol N L^{-1} d^{-1}). These rates are low compared to offshore waters in this region (Mulholland et al. 2019) and to oligotrophic inverse estuaries without a freshwater input (up to 64 nmol N L^{-1} d^{-1}; Messer et al. 2021), but, as noted above, in the range of those measured in relatively nitrogen-rich tropical and temperate estuaries (Fan et al. 2015; Bentzon-Tilia et al. 2015*b*; Ahmed et al. 2017). The average N_2 fixation rate in our study (1.48 nmol N L^{-1} d^{-1}) extrapolated to the study period (100 d), and multiplied by the mid tide volume of Narragansett Bay (https://www.savebay.org/bay_issues/facts-figures/; last accessed 16 June, 2021), would introduce 384 ± 494 mol N yr^{-1} to Narragansett Bay. This corresponds to < 1% of the diazotrophic nitrogen input estimated for the bay's sediments (Fulweiler et al. 2007) and < 0.5% of the yearly nitrogen load from land (Narragansett Bay Estuary Program 2017). A similar calculation for a nutrient-rich Danish estuary showed that N_2 fixation represented 5% of the nitrogen coming from land (Bentzon-Tilia et al. 2015*b*).

Conclusions

Our study suggests that pelagic N_2 fixation in Narragansett Bay is dominated by non-cyanobacterial diazotrophs of benthic origin. While the measured N_2 fixation rates were substantial as compared to previous open ocean measurements and in the range observed in similar estuarine systems, diazotrophic activity was well below previous estimates of benthic N_2 fixation, which can represent 20% to 40% of anthropogenic loading in Narragansett Bay (Fulweiler et al. 2007). We speculate that in nitrogen stressed estuaries like Narragansett Bay, pelagic N_2 fixation plays a minor role in reactive nitrogen supply. However, as environmental policies push toward reduced anthropogenic nutrient loading, diazotroph-derived nitrogen in estuarine systems such as Narragansett Bay may increase in the decades to come. Given that

estuarine systems make up 22% of the global coastline (Dürr et al. 2011), the export of nitrogen fixed via N_2 fixation to adjacent and nitrogen limited shelf waters may influence coastal productivity at a global scale.

References

Ahmed, A., M. Gauns, S. Kurian, P. Bardhan, A. Pratihary, H. Naik, D. M. Shenoy, and S. W. A. Naqvi. 2017. Nitrogen fixation rates in the eastern Arabian Sea. Estuar. Coast. Shelf Sci. **191**: 74–83. doi:10.1016/j.ecss.2017.04.005

Ahmed, A., N. Hema, S. A. Sarvesh, B. Pratirupa, G. Mangesh, N. Bhagyashri, and Naqvi, S. W. A. 2019. "nitrogen fixation and carbon uptake in a tropical estuarine system of goa, western india." Journal of Sea Research **144**: 16–21. doi:10.1016/j.seares.2018.09.018.

Angel, R., M. Nepel, C. Panhölzl, H. Schmidt, C. W. Herbold, S. A. Eichorst, and D. Woebken. 2018. Evaluation of primers targeting the diazotroph functional gene and Development of NifMAP—A bioinformatics pipeline for analyzing *nifH* amplicon data. Front. Microbiol. **9**: 1–15. doi:10.3389/fmicb.2018.00703

Benavides, M., P. H. Moisander, H. Berthelot, T. Dittmar, O. Grosso, and S. Bonnet. 2015. Mesopelagic N_2 fixation related to organic matter composition in the Solomon and Bismarck seas (Southwest Pacific). PLoS One **10**: e0143775. doi:10.1371/journal.pone.0143775

Bentzon-Tilia, M., H. Farnelid, K. Jürgens, and L. Riemann. 2014. Cultivation and isolation of N_2-fixing bacteria from suboxic waters in the Baltic Sea. FEMS Microbiol. Ecol. **88**: 358–371. doi:10.1111/1574-6941.12304

Bentzon-Tilia, M., I. Severin, L. H. Hansen, and L. Riemann. 2015*a*. Genomics and ecophysiology of heterotrophic nitrogen-fixing bacteria isolated from estuarine surface water. mBio **6**: e00929–e00915. doi:10.1128/mBio.00929-15

Bentzon-Tilia, M., S. J. Traving, M. Mantikci, H. Knudsen-Leerbeck, J. L. Hansen, S. Markager, and L. Riemann. 2015*b*. Significant N_2 fixation by heterotrophs, photoheterotrophs and heterocystous cyanobacteria in two temperate estuaries. ISME J. **9**: 273–285. doi:10.1038/ismej.2014.119

Bergondo, D. L., D. R. Kester, H. E. Stoffel, and W. L. Woods. 2005. Time-series observations during the low sub-surface oxygen events in Narragansett Bay during summer 2001. Mar. Chem. **97**: 90–103. doi:10.1016/j.marchem.2005.01.006

Bertics, V. J., C. R. Löscher, I. Salonen, A. W. Dale, J. Gier, R. A. Schmitz, and T. Treude. 2013. Occurrence of benthic microbial nitrogen fixation coupled to sulfate reduction in the seasonally hypoxic Eckernförde Bay, Baltic Sea. Biogeosciences **10**: 1243–1258. doi:10.5194/bg-10-1243-2013

Bombar, D., R. W. Paerl, and L. Riemann. 2016. Marine non-cyanobacterial diazotrophs: Moving beyond molecular detection. Trends Microbiol. **24**: 916–927. doi:10.1016/j.tim.2016.07.002

Bombar, D., R. W. Paerl, R. Anderson, and L. Riemann. 2018. Filtration via conventional glass fiber filters in 15n2 tracer assays fails to capture all nitrogen-fixing prokaryotes. Frontiers in Marine Science **5**: 6. doi:10.3389/fmars.2018.00006

Brown, S. M., and B. D. Jenkins. 2014. Profiling gene expression to distinguish the likely active diazotrophs from a sea of genetic potential in marine sediments. Environ. Microbiol. **16**: 3128–3142. doi:10.1111/1462-2920.12403

Buchfink, B., C. Xie, and D. H. Huson. 2014. Fast and sensitive protein alignment using DIAMOND. Nat. Methods **12**: 59–60. doi:10.1038/nmeth.3176

Cabello, A. M., K. A. Turk-Kubo, K. Hayashi, L. Jacobs, R. M. Kudela, and J. P. Zehr. 2020. Unexpected presence of the nitrogen-fixing symbiotic cyanobacterium UCYN-A in Monterey Bay, California. J. Phycol **56**: 1521–1533. doi:10.1111/jpy.13045

Callahan, B. J., P. J. McMurdie, M. J. Rosen, A. W. Han, A. J. A. Johnson, and S. P. Holmes. 2016. DADA2: High-resolution sample inference from Illumina amplicon data. Nat. Methods **13**: 581–583. doi:10.1038/nmeth.3869

Chakraborty, S., K. H. Andersen, A. W. Visser, K. Inomura, M. J. Follows, and L. Riemann. 2021. Quantifying nitrogen fixation by heterotrophic bacteria in sinking marine particles. Nat. Commun. **12**: 4085. doi:10.1038/s41467-021-23875-6

Clarke, K. R., R. N. Gorley, P. J. Somerfield, and R. M. Warwick. 2014. Change in marine communities: An approach to statistical analysis and interpretation, 3rd ed. Primer-E Ltd.

Codiga, D. L., H. E. Stoffel, C. F. Deacutis, S. Kiernan, and C. A. Oviatt. 2009. Narragansett Bay hypoxic event characteristics based on fixed-site monitoring network time series: Intermittency, geographic distribution, spatial synchronicity, and interannual variability. Estuar. Coasts **32**: 621–641. doi:10.1007/s12237-009-9165-9

Cornwell, J. C., W. M. Kemp, and T. M. Kana. 1999. Denitrification in coastal ecosystems: Methods, environmental controls, and ecosystem level controls, a review. Aquat. Ecol. **33**: 41–54. doi:10.1023/A:1009921414151

Dabundo, R., M. F. Lehmann, L. Treibergs, C. R. Tobias, M. A. Altabet, P. H. Moisander, and J. Granger. 2014. The contamination of commercial $^{15}N_2$ gas stocks with ^{15}N-labeled nitrate and ammonium and consequences for nitrogen fixation measurements. PLoS One **9**: e110335. doi:10.1371/journal.pone.0110335

Dürr, H. H., G. G. Laruelle, C. M. van Kempen, C. P. Slomp, M. Meybeck, and H. Middelkoop. 2011. Worldwide typology of nearshore coastal systems: Defining the estuarine filter of river inputs to the oceans. Estuar. Coasts **34**: 441–458. doi:10.1007/s12237-011-9381-y

Fan, H., H. Bolhuis, and L. J. Stal. 2015. Drivers of the dynamics of diazotrophs and denitrifiers in North Sea bottom

waters and sediments. Front. Microbiol. **6**: 1–13. doi:10.3389/fmicb.2015.00738

Farnelid, H., K. Turk-Kubo, M. Del Carmen Muñoz-Marín, and J. P. Zehr. 2016. New insights into the ecology of the globally significant uncultured nitrogen-fixing symbiont UCYN-A. Aquat. Microb. Ecol. **77**: 128–138. doi:10.3354/ame01794

Frank, I. E., K. A. Turk-Kubo, and J. P. Zehr. 2016. Rapid annotation of *nifH* gene sequences using classification and regression trees facilitates environmental functional gene analysis. Environ. Microbiol. Rep. **8**: 905–916. doi:10.1111/1758-2229.12455

Fulweiler, R. W., S. W. Nixon, B. A. Buckley, and S. L. Granger. 2007. Reversal of the net dinitrogen gas flux in coastal marine sediments. Nature **448**: 180–182. doi:10.1038/nature05963

Fulweiler, R. W., S. M. Brown, S. W. Nixon, and B. D. Jenkins. 2013. Evidence and a conceptual model for the co-occurrence of nitrogen fixation and denitrification in heterotrophic marine sediments. Mar. Ecol. Prog. Ser. **482**: 57–68. doi:10.3354/meps10240

Geisler, E., B. Anne, B.-Z. Edo, and R. Eyal. 2020. "Heterotrophic nitrogen fixation at the hyper-eutrophic qishon river and estuary system." Frontiers in Microbiology **11**: 1370. doi:10.3389/fmicb.2020.01370.

Gradoville, M. R., D. Bombar, B. C. Crump, R. M. Letelier, J. P. Zehr, and A. E. White. 2017. Diversity and activity of nitrogen-fixing communities across ocean basins. Limnol. Oceanogr. **62**: 1895–1909. doi:10.1002/lno.10542

Guasch, H., J. Armengol, E. Martí, and S. Sabater. 1998. Diurnal variation in dissolved oxygen and carbon dioxide in two low-order streams. Water Res. **32**: 1067–1074. doi:10.1016/S0043-1354(97)00330-8

Guizien, K., C. Dupuy, P. Ory, H. Montanié, H. Hartmann, M. Chatelain, and M. Karpytchev. 2014. Microorganism dynamics during a rising tide: Disentangling effects of resuspension and mixing with offshore waters above an intertidal mudflat. J. Mar. Syst. **129**: 178–188. doi:10.1016/j.jmarsys.2013.05.010

Hagino, K., N. Tomioka, J. R. Young, Y. Takano, R. Onuma, and T. Horiguchi. 2016. Extracellular calcification of *Braarudosphaera bigelowii* deduced from electron microscopic observations of cell surface structure and elemental composition of pentaliths. Mar. Micropaleontol. **125**: 85–94. doi:10.1016/j.marmicro.2016.04.002

Hewson, I., P. H. Moisander, A. E. Morrison, and J. P. Zehr. 2007. Diazotrophic bacterioplankton in a coral reef lagoon: Phylogeny, diel nitrogenase expression and response to phosphate enrichment. ISME J. **1**: 78–91. doi:10.1038/ismej.2007.5

Howarth, R. W., R. Marino, and J. J. Cole. 1988. Nitrogen fixation in freshwater, estuarine, and marine ecosystems. 2. Rates and importance. Limnol. Oceanogr. **33**: 688–701. doi:10.4319/lo.1988.33.4part2.0669

Hutchins, D. A., and F. Fu. 2017. Microorganisms and ocean global change. Nat. Microbiol. **2**: 17058. doi:10.1038/nmicrobiol.2017.58

Jayaswal, V., T. K. F. Wong, J. Robinson, L. Poladian, and L. S. Jermiin. 2014. Mixture models of nucleotide sequence evolution that account for heterogeneity in the substitution process across sites and across lineages. Syst. Biol. **63**: 726–742. doi:10.1093/sysbio/syu036

Karl, D. M., M. J. Church, J. E. Dore, R. M. Letelier, and C. Mahaffey. 2012. Predictable and efficient carbon sequestration in the North Pacific Ocean supported by symbiotic nitrogen fixation. Proc. Natl. Acad. Sci. **109**: 1842–1849. doi:10.1073/pnas.1120312109

Katoh, K., J. Rozewicki, and K. D. Yamada. 2018. MAFFT online service: Multiple sequence alignment, interactive sequence choice and visualization. Brief. Bioinform. **20**: 1160–1166. doi:10.1093/bib/bbx108

Kozlov, A. M., D. Darriba, T. Flouri, B. Morel, A. Stamatakis, and J. Wren. 2019. RAxML-NG: A fast, scalable and user-friendly tool for maximum likelihood phylogenetic inference. Bioinformatics **35**: 4453–4455. doi:10.1093/bioinformatics/btz305

Landolfi, A., P. Kähler, W. Koeve, and A. Oschlies. 2018. Global marine N_2 fixation estimates: From observations to models. Front. Microbiol. **9**: 2112. doi:10.3389/fmicb.2018.02112

Letunic, I., and P. Bork. 2019. Interactive tree of life (iTOL) v4: Recent updates and new developments. Nucleic Acids Res. **47**: 256–259. doi:10.1093/nar/gkz239

Li, Y., and T. J. Smayda. 1998. Temporal variability of chlorophyll in Narragansett Bay, 1973–1990. ICES J. Mar. Sci. **55**: 661–667. doi:10.1006/jmsc.1998.0383

Luo, Y.-W., and others. 2012. Database of diazotrophs in global ocean: Abundance, biomass and nitrogen fixation rates. Earth Syst. Sci. Data **4**: 47–73. doi:10.5194/essd-4-47-2012

Mahaffey, C., A. F. Michaels, and D. G. Capone. 2005. The conundrum of marine N2 fixation. Am. J. Sci. **305**: 546–595. doi:10.2475/ajs.305.6-8.546

Marino, R., F. Chan, R. W. Howarth, M. Pace, and G. E. Likens. 2002. Ecological and biogeochemical interactions constrain planktonic nitrogen fixation in estuaries. Ecosystems **5**: 719–725. doi:10.1007/s10021-002-0176-7

McMurdie, P. J., and S. Holmes. 2013. Phyloseq: An R package for reproducible interactive analysis and graphics of microbiome census data. PLoS One **8**: e61217. doi:10.1371/journal.pone.0061217

Messer, L. F., M. V. Brown, P. D. Van Ruth, M. Doubell, and J. R. Seymour. 2021. Temperate southern Australian coastal waters are characterised by surprisingly high rates of nitrogen fixation and diversity of diazotrophs. PeerJ **9**: 1–32. doi:10.7717/peerj.10809

Moisander, P. H., A. E. Morrison, B. B. Ward, B. D. Jenkins, and J. P. Zehr. 2007. Spatial-temporal variability in diazotroph assemblages in Chesapeake Bay using an oligonucleotide *nifH* microarray. Environ. Microbiol. **9**: 1823–1835. doi:10.1111/j.1462-2920.2007.01304.x

Moisander, P. H., R. A. Beinart, M. Voss, and J. P. Zehr. 2008. Diversity and abundance of diazotrophic microorganisms in the South China Sea during intermonsoon. ISME J. **2**: 954–967. doi:10.1038/ismej.2008.51

Moisander, P. H., T. Serros, R. W. Paerl, R. A. Beinart, and J. P. Zehr. 2014. Gammaproteobacterial diazotrophs and *nifH* gene expression in surface waters of the South Pacific Ocean. ISME J. **8**: 1962–1973. doi:10.1038/ismej.2014.49

Moreira-Coello, V., B. Mouriño-Carballido, E. Marañón, A. Fernández-Carrera, M. Pérez-Lorenzo, and A. Bode. 2019. Quantifying the overestimation of planktonic N_2 fixation due to contamination of $^{15}N_2$ gas stocks. J. Plankton Res. **41**: 567–570. doi:10.1093/plankt/fbz034

Moynihan, M. 2020. nifHdada2 GitHub repository. doi:10.5281/zenodo.3958370

Mulholland, M. R., and others. 2012. Rates of dinitrogen fixation and the abundance of diazotrophs in North American coastal waters between Cape Hatteras and Georges Bank. Limnol. Oceanogr. **57**: 1067–1083. doi:10.4319/lo.2012.57.4.1067

Mulholland, M. R., P. W. Bernhardt, B. N. Widner, C. R. Selden, P. D. Chappell, S. Clayton, A. Mannino, and K. Hyde. 2019. High rates of N_2 fixation in temperate, Western North Atlantic coastal waters expand the realm of marine diazotrophy. Global Biogeochem. Cycles **33**: 826–840. doi:10.1029/2018GB006130

Narragansett Bay Estuary Program. 2017. State of Narragansett Bay and its watershed (Chapter 8: Nutrient loading. p. 166–189). Technical Report. Providence, RI.

Nixon, S. W., and others. 1996. The fate of nitrogen and phosphorus at the land-sea margin of the North Atlantic Ocean. Biogeochemistry **35**: 141–180. doi:10.1007/BF02179826

Nixon, S. W., B. Buckley, S. Granger, L. Harris, A. Oczkowski, L. Cole, and R. Fulweiler. 2005. Anthropogenic nutrient inputs to Narragansett Bay: A twenty-five year perspective. Report to The Narragansett Bay commission and Rhode Island Sea Grant.

Nixon, S. W., R. W. Fulweiler, B. A. Buckley, S. L. Granger, B. L. Nowicki, and K. M. Henry. 2009. The impact of changing climate on phenology, productivity, and benthic-pelagic coupling in Narragansett Bay. Estuar. Coast. Shelf Sci. **82**: 1–18. doi:10.1016/j.ecss.2008.12.016

Oczkowski, A. others 2018. How the distribution of anthropogenic nitrogen has changed in Narragansett Bay (RI, USA) following major reductions in nutrient loads. Estuar. Coasts **41**: 2260–2276. doi:10.1007/s12237-018-0435-2

Oksanen, J., and others. 2019. vegan: Community ecology package. R package version 2.5-2. Cran R.

Oviatt, C., A. Keller, and L. Reed. 2002. Annual primary production in Narragansett Bay with no bay-wide winter-spring phytoplankton bloom. Estuar. Coast. Shelf Sci. **54**: 1013–1026. doi:10.1006/ecss.2001.0872

Oviatt, C., L. Smith, J. Krumholz, C. Coupland, H. Stoffel, A. Keller, M. C. McManus, and L. Reed. 2017. Managed nutrient reduction impacts on nutrient concentrations, water clarity, primary production, and hypoxia in a north temperate estuary. Estuar. Coast. Shelf Sci. **199**: 25–34. doi:10.1016/j.ecss.2017.09.026

Pedersen, J. N., D. Bombar, R. W. Paerl, and L. Riemann. 2018. Diazotrophs and N_2-fixation associated with particles in coastal estuarine waters. Front. Microbiol. **9**: 2759. doi:10.3389/fmicb.2018.02759

Porter, E. T., R. P. Mason, and L. P. Sanford. 2010. Effect of tidal resuspension on benthic-pelagic coupling in an experimental ecosystem study. Mar. Ecol. Prog. Ser. **413**: 33–53. doi:10.3354/meps08709

Revelle, W. 2021. Psych: Procedures for psychological, psychometric, and personality research.

Riemann, L., H. Farnelid, and G. F. Steward. 2010. Nitrogenase genes in non-cyanobacterial plankton: Prevalence, diversity and regulation in marine waters. Aquat. Microb. Ecol. **61**: 235–247. doi:10.3354/ame01431

Rogers, J. 2008. Circulation and transport in the heart of Narragansett Bay. Univ. of Rhode Island.

Severin, I., M. Bentzon-tilia, P. H. Moisander, and L. Riemann. 2015. Nitrogenase expression in estuarine bacterioplankton influenced by organic carbon and availability of oxygen. FEMS Microbiol. Lett. **362**: 1–26.

Short, S. M., B. D. Jenkins, and J. P. Zehr. 2004. Spatial and temporal distribution of two diazotrophic bacteria in the Chesapeake Bay. Appl. Environ. Microbiol. **70**: 2186–2192. doi:10.1128/AEM.70.4.2186-2192.2004

Short, S. M., and J. P. Zehr. 2007. Nitrogenase gene expression in the Chesapeake Bay estuary. Environ. Microbiol. **9**: 1591–1596. doi:10.1111/j.1462-2920.2007.01258.x

Spinette, R. F., S. M. Brown, A. L. Ehrlich, G. Puggioni, C. Deacutis, and B. D. Jenkins. 2019. Diazotroph activity in surface Narragansett Bay sediments in summer is stimulated by hypoxia and organic matter delivery. Mar. Ecol. Prog. Ser. **614**: 35–50. doi:10.3354/meps12901

Subramaniam, A., and others. 2008. "Amazon River Enhances Diazotrophy and Carbon Sequestration in the Tropical North Atlantic Ocean." Proceedings of the National Academy of Sciences **105**: 10460–10465. doi:10.1073/pnas.0710279105.

Tang, W., and others. 2019. Revisiting the distribution of oceanic N_2 fixation and estimating diazotrophic contribution to marine production. Nat. Commun. **10**: 1–10. doi:10.1038/s41467-019-08640-0

Thompson, A., B. J. Carter, K. Turk-Kubo, F. Malfatti, F. Azam, and J. P. Zehr. 2014. Genetic diversity of the unicellular nitrogen-fixing cyanobacteria UCYN-A and its prymnesiophyte host. Environ. Microbiol. **16**: 3238–3249. doi:10.1111/1462-2920.12490

Torgo, L. 2016. Data mining with R, learning with case studies, 2nd ed. Chapman and Hall/CRC.

Turk-Kubo, K. A., H. M. Farnelid, I. N. Shilova, B. Henke, and J. P. Zehr. 2017. Distinct ecological niches of marine

symbiotic N_2-fixing cyanobacterium *Candidatus Atelocyanobacterium thalassa* sublineages. J. Phycol. **53**: 451–461. doi:10.1111/jpy.12505

Vihtakari, M. 2020. ggOceanMaps: Plot Data on Oceanographic Maps using "ggplot2".

Wang, Q., J. F. I. Quensen, J. A. Fish, T. K. Lee, Y. Sun, J. M. Tiedje, and J. R. Cole. 2013. Ecological patterns of *nifH* genes in four terrestrial climatic zones explored with targeted metagenomics using FrameBot, a new informatics tool. mBio **4**: 1–9. doi:10.1128/mBio.00592-13.Editor

White, A. E., and others. 2020. A critical review of the $^{15}N_2$ tracer method to measure diazotrophic production in pelagic ecosystems. Limnol. Oceanogr. Methods **18**: 129–147. doi:10.1002/lom3.10353

Wickham, H. 2016. ggplot2: Elegant graphics for data analysis. Springer-Verlag.

Zehr, J. P., and P. J. Turner. 2001. Nitrogen fixation: Nitrogenase genes and gene expression, p. 271–286. *In* Methods in microbiology. Academic Press. **30**. doi:10.1016/S0580-9517(01)30049-1

Zehr, J. P., B. D. Jenkins, S. M. Short, and G. F. Steward. 2003. Nitrogenase gene diversity and microbial community structure: A cross-system comparison. **5**: 539–554.

Zilius, M., A. Samuiloviene, R. Stanislauskien□, E. Broman, S. Bonaglia, R. Meškys, and A. Zaiko. 2020. Depicting temporal, functional, and phylogenetic patterns in estuarine diazotrophic communities from environmental DNA and RNA. Microb. Ecol. **81**: 36–51. doi:10.1007/s00248-020-01562-1

Acknowledgments

We are indebted to C. Oviatt, H. Stoffel, E. Requintina, K. Huizenga, J. Jacques, E. Zanzarov, and L. Reed from the Marine Ecosystems Research Laboratory (MERL) at the University of Rhode Island's Graduate School of Oceanography for their invaluable help with sampling and for providing the data for inorganic nutrients, chlorophyll concentrations and hydrographic parameters. We also thank K. Shoemaker, R. Nuttall, and A. Profetto for their support with sample processing at UMD. In addition, we thank R.W. Fulweiler for her insightful comments on a previous version of this manuscript and acknowledge the comprehensive and detailed comments of two anonymous reviewers. S.H., M.B., E.S., and L.R. were supported by grant 6108-00013 from the Danish Council for independent research to L.R. P.M. was supported by NSF OCE 1733610. CE was supported through an NSF-REU program DBI1460980 at UMD.

Conflict of interest

None declared.

Submitted 27 July 2021
Revised 22 November 2021
Accepted 28 November 2021

Associate editor: Laura Bristow